POSSIBLE WEIGHTING SCHEMES FOR GPS CARRIER PHASE OBSERVATIONS IN THE PRESENCE OF MULTIPATH

by

J. P. Collins and R. B. Langley

Geodetic Research Laboratory
Department of Geodesy and Geomatics Engineering
University of New Brunswick
Fredericton, N.B.
Canada
E3B 5A3

for

The United States Army Corps of Engineers Topographic Engineering Center

March 1999

Contract No. DAAH04-96-C-0086
TCN 98151
Scientific Services Program

REPORT DOCUMENTATION PAGE

Form Approved
OMB No. 0704-0188

1. AGENCY USE ONLY *(Leave Blank)*	2. REPORT DATE	3. REPORT TYPE AND DATES COVERED
	March 1999	Final Report; From: 10 98 To: 03 99

4. TITLE AND SUBTITLE
Possible Weighting Schemes for GPS Carrier Phase Observations in the Presence of Multipath

5. FUNDING NUMBERS
Contract DAAH04–96–C–0086

6. AUTHORS
J.P. Collins
R.B. Langley

7. PERFORMING ORGANIZATION NAME(S) AND ADDRESS(ES)
Geodetic Research Laboratory
Department of Geodesy and Geomatics Engineering
University of New Brunswick
Fredericton, N.B., Canada, E3B 5A3

8. PERFORMING ORGANIZATION REPORT NUMBER
Delivery Order 0334

9. SPONSORING / MONITORING AGENCY NAME(S) AND ADDRESS(ES)
U. S. Army Research Office
P. O. Box 12211
Research Triangle Park, NC 27709

10. SPONSORING / MONITORING AGENCY REPORT NUMBER
TCN 98151

11. SUPPLEMENTARY NOTES
Task was performed under a Scientific Services Agreement issued by Battelle, Research Triangle Park Office, 200 Park Drive, P. O. Box 12297, NC 27709.

12a. DISTRIBUTION / AVAILABILITY STATEMENT
May not be released by other than sponsoring organization without approval of U.S. Army Research Office.

12b. DISTRIBUTION CODE

13. ABSTRACT *(Maximum 200 words)*

Three possible weighting schemes that can be used with GPS carrier phase observables have been tested. The aim was to achieve consistent millimetre-level accuracy of coordinate determinations in the presence of multipath. The three weighting schemes are: 1) equal weighting of all carrier phase observations; 2) weighting using the cosecant of the satellite elevation angle; and 3) weighting using Trimble receiver generated signal-to-noise (SNR) values. Only the first scheme is generally available in commercial GPS processing software. All three are implemented in the University of New Brunswick's Differential Positioning Package (DIPOP) software, which was used to test the effectiveness of each scheme on several large data sets recorded on a small network at an earth dam structure monitored by the U.S. Army Corps of Engineers.

The cosecant and SNR weighting schemes provide a significant improvement over the equal-weighting scheme. With their use, vertical repeatability at the level of several millimetres is possible over observation sessions as short as 10 minutes in length. At the same time, ambiguities can be fixed over a greater range of a-priori coordinate uncertainties. Nevertheless, the difference in height between individual observation sessions and weighting schemes can approach the centimetre level due to poor geometry and data outliers. It has been determined that the cosecant and SNR weighting schemes are almost numerically equivalent due to the scaling effect of the a-posteriori variance factor. Hence, an observation weighting scheme using SNR values from, for example, Trimble receivers may not be absolutely necessary for ultra-precise structure monitoring.

14. SUBJECT TERMS
GPS, data processing, small geodetic networks, deformation monitoring, multipath

15. NUMBER OF PAGES
vi, 33

16. PRICE CODE

17. SECURITY CLASSIFICATION OF REPORT	18. SECURITY CLASSIFICATION OF THIS PAGE	19. SECURITY CLASSIFICATION OF ABSTRACT	20. LIMITATION OF ABSTRACT

ABSTRACT

Three possible weighting schemes that can be used with GPS carrier phase observables have been tested. The aim was to achieve consistent millimetre-level accuracy of coordinate determinations in the presence of multipath. The three weighting schemes are: 1) equal weighting of all carrier phase observations; 2) weighting using the cosecant of the satellite elevation angle; and 3) weighting using Trimble receiver generated signal-to-noise (SNR) values. Only the first scheme is generally available in commercial GPS processing software. All three are implemented in the University of New Brunswick's Differential Positioning Package (DIPOP) software, which was used to test the effectiveness of each scheme on several large data sets recorded on a small network at an earth dam structure monitored by the U.S. Army Corps of Engineers.

The cosecant and SNR weighting schemes provide a significant improvement over the equal-weighting scheme. With their use, vertical repeatability at the level of several millimetres is possible over observation sessions as short as 10 minutes in length. At the same time, ambiguities can be fixed over a greater range of *a-priori* coordinate uncertainties. Nevertheless, the difference in height between individual observation sessions and weighting schemes can approach the centimetre level due to poor geometry and data outliers. It has been determined that the cosecant and SNR weighting schemes are almost numerically equivalent due to the scaling effect of the *a-posteriori* variance factor. Hence, an observation weighting scheme using SNR values from, for example, Trimble receivers may not be absolutely necessary for ultra-precise structure monitoring.

TABLE OF CONTENTS

LIST OF FIGURES

LIST OF TABLES

ACKNOWLEDGEMENTS

This work was supported by the Topographic Engineering Center (Mr. James C. Eichholz) under the auspices of the U.S. Army Research Office Scientific Services Program administered by Battelle (Delivery Order 0334, Contract No. DAAH04-96-C-0086).

1. INTRODUCTION

The Department of Geodesy and Geomatics Engineering was contracted by the United States Army Corps of Engineers to further investigate the use of the satellite-based Global Positioning System (GPS) for structural movement studies. The focus of the investigation was to determine if a suitable weighting scheme could be used to minimise the impact of site-specific multipath errors on the GPS carrier phase measurements. This report presents the results of the work and recommends further avenues of study.

The remainder of this section details the weighting schemes used and outlines the data set processed. The philosophy behind the weighting schemes is described. Section two describes the tests undertaken with the data set and the results obtained. Section three details our conclusions and recommendations.

1.1. Potential Weighting Schemes

The usual method for weighting GPS carrier phase data, other than using equal weights, is to use a function of the satellite elevation angle recorded by the observing station. The most common function used is the tropospheric mapping function (TMF) that scales the neutral-atmosphere signal delay from the zenith direction to the satellite elevation angle. The theory behind its use is that the tropospheric delay error increases towards the horizon (due to its short-distance correlation), as does the amount of noise inherent to the GPS signals. In effect, the statistical variance of the signal noise is assumed to be proportional to the squared value of the TMF.

While we expect the tropospheric error to cancel almost completely over short baselines, the signal noise will remain and use of the TMF is still justified. Figure 1 shows the TMF as computed by the Black and Eisner function $1.001/[0.002001 + \sin^2(e)]^{1/2}$ [*Black and Eisner*, 1984], and as computed by the cosecant function of the elevation angle $1/\sin(e)$. As Figure 1 indicates, the cosecant function can be used as a first-order approximation to the TMF, as it diverges from it by only ~12% at most (at an elevation angle of 5°). Hence, this is the function we have used as the elevation angle weighting function.

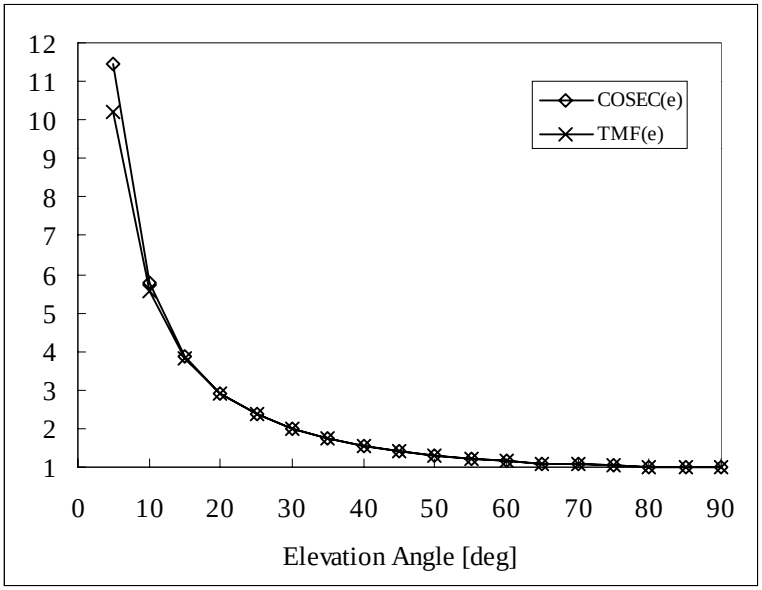

Figure 1. Potential weighting functions as a function of satellite elevation angle.

An alternative, and potentially more powerful, weighting function can be derived directly from measurements of the quality of each carrier phase measurement. This information is contained in the signal-to-noise ratio (SNR), should the GPS receiver provide it. The SNR is usually represented in terms of the carrier-to-noise-power-density

ratio, C/N_0. This is the ratio of the power level of the signal carrier to the noise power in a one hertz bandwidth. A typical value is 45 dB-Hz, although actual values will vary due to multipath, the receiver antenna's gain pattern, and to a lesser extent, satellite transmission level differences and atmospheric attenuation effects.

Despite the fact that the potential merits of using the SNR information as a weighting scheme was discussed some time ago [*Talbot*, 1988], it seems that a comprehensive examination of the technique has only taken place recently [*Hartinger and Brunner*, 1998]. The use of the SNR information can be seen as an intermediate step between the simple functional models, such as the TMF, usually used to weight GPS observations, and the more complicated stochastic methods that are beginning to be investigated (e.g., *Tiberius et al.*, [1999]). These techniques require as much information as possible about the stochastic quantities of the observables to construct a fully populated variance-covariance matrix.

Several researchers have also investigated the use of SNR information to compute multipath corrections to the phase data [*Axelrad et al.*, 1994; *Comp and Axelrad*, 1996], however these techniques are generally very complex, involving spectral decomposition to reveal component multipath signals. As such, their implementation is beyond the scope of this investigation, however software to implement what appears to be a similar technique is available freely from the Internet [*Herring*, 1998].

The equation for approximating the error on the carrier phase (L1 or L2) has been given by, e.g., *Langley* [1997] and *Braasch and Van Dierendonck* [1999]:

$$\sigma_{L1,\,L2}\,(\mathrm{m}) = \sqrt{\frac{B}{c/n_0}} \cdot \frac{\lambda}{2\pi}, \qquad (1)$$

where B is the carrier tracking loop bandwidth (Hz), λ is the wavelength of the carrier (m) and c/n_0 is the carrier-to-noise density expressed as a ratio (= $10^{\frac{C/N_0}{10}}$ for C/N_0 expressed in dB-Hz). This equation gives a nominal value for the L1 carrier phase noise of 0.2 millimetre for a 2 Hz bandwidth loop and a C/N_0 value of 45 dB-Hz.

Provided that the C/N_0 values can be recovered from the GPS receiver, equation (1) should provide a near-optimum way of weighting the carrier phase observations. It should be noted that a weighting scheme based on equation (1) ignores any contribution to the phase noise from the local oscillator and is only strictly valid for relatively strong signals well above the tracking threshold of the receiver.

The only problem precluding the use of equation (1) is the recovery of a receiver's SNR information. Currently, manufacturers are not obliged to provide SNR (or C/N_0) values and those that do often provide them in a reduced, proprietary, format. There are discussions currently underway on how to standardise the reporting of SNR values with a view to including them into the specifications of the RINEX format of GPS observation files [*Estey*, 1998; *anon.*, 1998].

For the purposes of this study, we have used the values labelled 'L1 signal/noise counts' provided by Trimble geodetic receivers as being equivalent to C/N_0 values. These are the values currently output by the translation software 'teqc' into RINEX format

[*Estey*, 1998]. Figure 2 gives an example of the SNR output from a Trimble geodetic receiver. This plot represents data from a satellite (PRN 02) that passes nearly overhead, during which time the SNR values are on the order of 30, lower than what we might expect if they are supposed to be C/N_0 values. The discrepancy is almost certainly the result of a proprietary scaling algorithm in this receiver and in other aspects the pattern resembles true C/N_0 values.

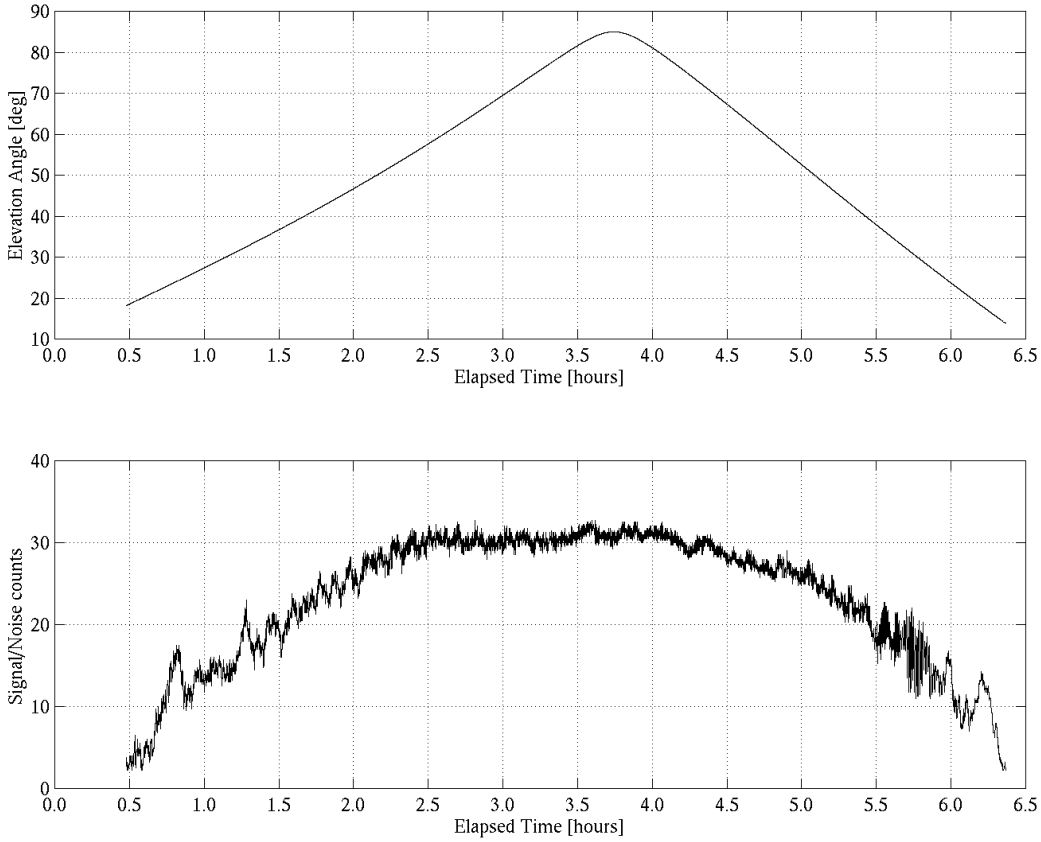

Figure 2. Example of satellite track and associated L1 Trimble "SNR" values.

1.2. The Data Set

The data used for this study consists of a portion of data recorded at an earth dam structure in East Lynn, West Virginia. The data was recorded using dual-frequency Trimble geodetic receivers at two reference stations on either side of the dam (SG and EL), a station on the crest of the dam (D3) and from two stations located on the upstream and downstream toes of the dam (UT and DT respectively). A summary of the data processed is given in Table 1. Several short sessions of data were recorded at a string of stations on the upstream and downstream sides of the crest of the dam (D1-D5, U1-U5). This portion of the data has not been processed in this study.

Table 1. Duration of observation sessions from stations occupied at East Lynn.

Station Name	DIPOP Code	Session 1	Session 2	Session 3
SG-2	SG	$3^h33^m46^s$	$3^h16^m12^s$	$3^h34^m47^s$
East Lynn	EL	$3^h20^m06^s$	$3^h01^m48^s$	$3^h41^m10^s$
Downstream Crest 3	D3	$10^h29^m32^s$	$4^h11^m47^s$	$0^h34^m29^s$*
Upstream Toe	UT	$10^h53^m40^s$	$4^h35^m51^s$	-n/a-
Downstream Toe	DT	11^h03^m43	$4^h03^m30^s$	-n/a-

*Recorded as a rapid-static session, not processed for this study.

The data was recorded to provide control between stations SG, EL and D3 and then to provide cross-sections from the crest to the upstream and downstream toe points.

1.3. Processing Technique

The data was processed using the UNB Differential Positioning Package (DIPOP) software, which uses double difference carrier phase observables to achieve ultra-precise positioning results. For this investigation, because of the small aperture of the network, broadcast ephemerides were used to compute the satellite positions. The L1 carrier phase observable was used throughout because of its superior noise characteristics over the L2 observable and the ionosphere-free linear combination. The L2 observations were used however, in the cycle slip detection portion of the double difference pre-processing. The ionospheric and tropospheric components of the double-difference range error were assumed to have completely cancelled, due to the short length of the baselines. All data was processed at the one second sampling interval recorded and with an elevation mask angle of 10 degrees.

Ambiguity resolution was done empirically by computing so-called “float” solutions from the longest extent of data available for each baseline, and then rounding to the nearest integer values. These control solutions were then re-computed to check the values were correct and to ensure that no cycle slips remained in the data. The ambiguities were stored and used for all processing of each particular baseline. Individual baselines were processed separately for this study; no network solutions were required.

2. RESULTS

Three weighting techniques have been tested in this study. The default scheme is that of weighting all observations equally. The two new schemes weight the observations by the cosecant of the elevation angle and by the SNR values. In all three schemes, the mathematical correlations due to using double-difference observations have been accounted for (see Appendix A for more details).

2.1. Control Points

The focus for the East Lynn processing was the cross-sections from station D3 to stations UT and DT. It was originally intended to provide control for station D3 by tying it to the only previously known point SG through the GPS data. However it was at this point we began to perceive the nature of the problem of weighting the GPS observations. All the data linking stations SG and D3 was used to compute a fix (see Table 1); the results are shown in Table 2.

The exceptionally small formal errors in Table 2 are a consequence of the long "integration time" of this solution (~10 hours, from all 3 sessions) and the high data collection rate. We can see immediately that the cosecant and SNR weighting schemes produce very similar results. The problem here lies in the fact that the coordinates from both these solutions are biased from those of the equal-weight solution. The difference in the height coordinates alone is over 1 cm. This result immediately indicates the problems of computing high precision coordinates from GPS observations. Even with a long data

arc, differences of the order of 1 cm are possible, due solely to the particular weighting scheme in use.

Table 2. Results of control processing for baseline SG-D3.
Solutions represent discrepancies from *a-priori* D3 coordinates.

Coordinates	Latitude (N)	Longitude (E)	Height (m)
SG (*fixed*)	38°08′44″.85091	–82°22′53″.15501	158.1660
D3 (*a-priori*)	38°08′41″.75408	–82°23′02″.74030	187.1580
Equal weight	0.5 ± 0.03 mm (1σ)	0.5 ± 0.02 mm (1σ)	27.3 ± 0.05 mm (1σ)
Cosecant wgt.	0.7 ± 0.02 mm (1σ)	1.4 ± 0.01 mm (1σ)	15.4 ± 0.04 mm (1σ)
SNR weight	0.5 ± 0.02 mm (1σ)	1.3 ± 0.01 mm (1σ)	15.6 ± 0.04 mm (1σ)

Given the short baseline in this case (253.84m), all errors apart from multipath should essentially cancel out and therefore the positions computed with the new weighted solutions will be more accurate. However, without an independent set of coordinates to provide a check, we cannot be absolutely sure. Similar results occur when trying to control station EL from station SG and when trying to establish control coordinates for stations UT and DT from station D3. Height differences on the order of 1 cm are consistently found between the equally weighted solutions and the cosecant and SNR weighted solutions. Given this situation, we concentrated on the potential level of repeatability obtainable with these weighting schemes.

2.2. Repeatability

We have taken the approximately 10 hours of data recorded on the D3-UT and D3-DT baselines and computed independent solutions using the various weighting schemes over sessions of progressively shorter periods of time. In each case station D3 was fixed to the coordinates resolved by the SNR weighted solution in Table 2. The carrier phase ambiguities were fixed to integer values from the control solutions described previously. The coordinates for stations DT and UT were estimated independently every 60, 30, 20, and 10 minutes throughout the whole data sets.

In the following figures, the north, east, vertical and baseline length differences for stations DT and UT are plotted for the four session lengths and the three solution types. Because we do not have "truth" coordinates for stations DT and UT, each component for each solution is corrupted by a constant bias. In order to provide a relative comparison between the types of solution, a constant value has been removed from each component's results. Therefore, only comparisons between the results of the three weighting schemes can be made.

The three solution types are represented in all the following figures with a dashed line (equal weights), a dashed-dot line (cosecant weights) and a solid line (SNR weights).

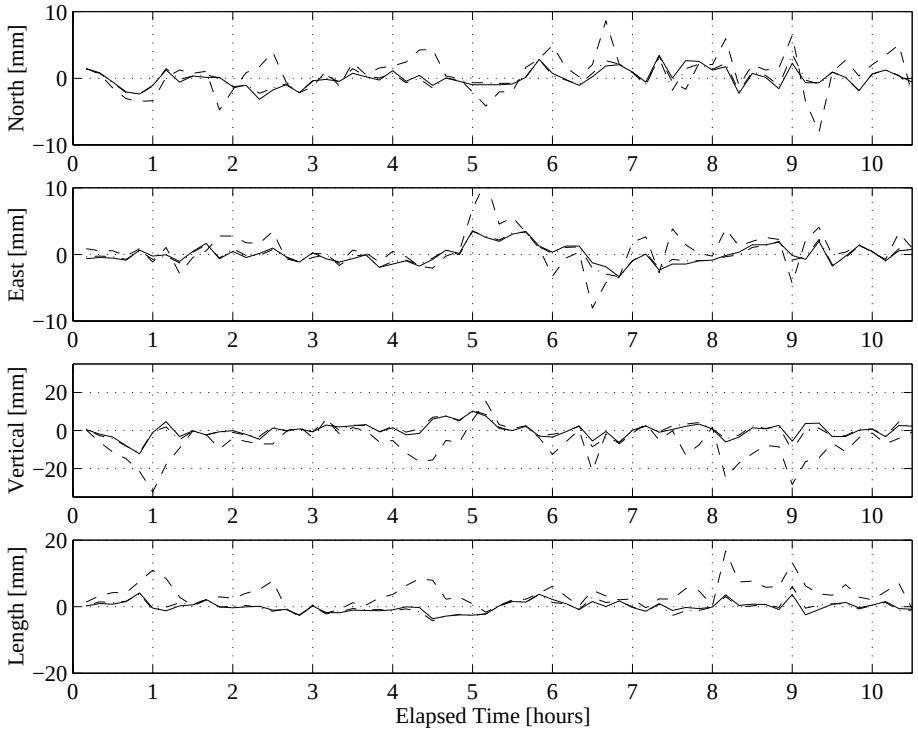

Figure 3. Repeated solutions of baseline D3-DT; length of sessions = 10 minutes.

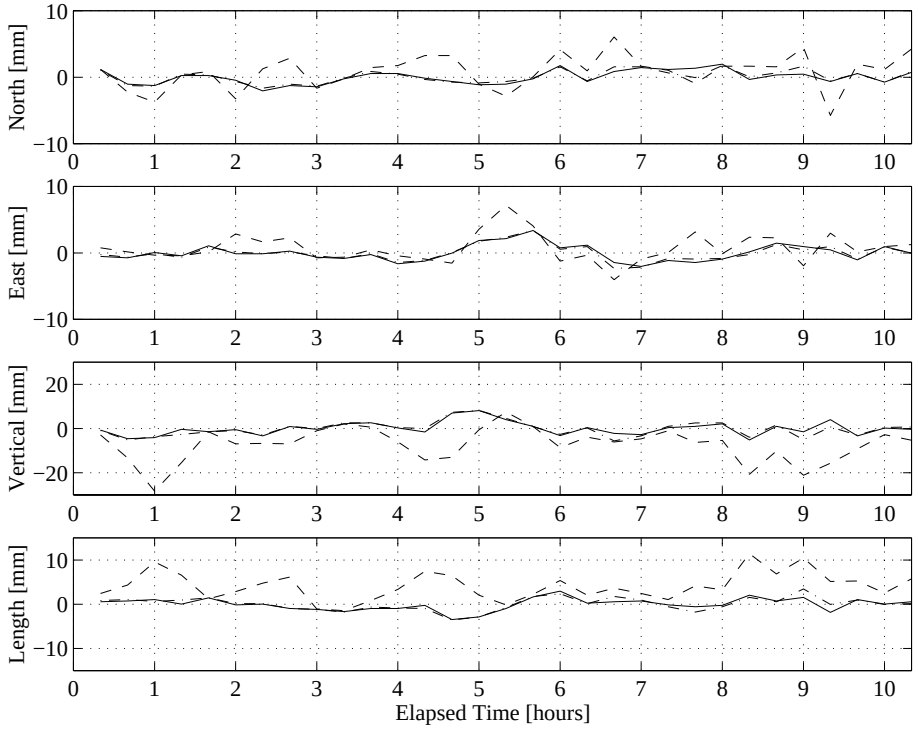

Figure 4. Repeated solutions of baseline D3-DT; length of sessions = 20 minutes.

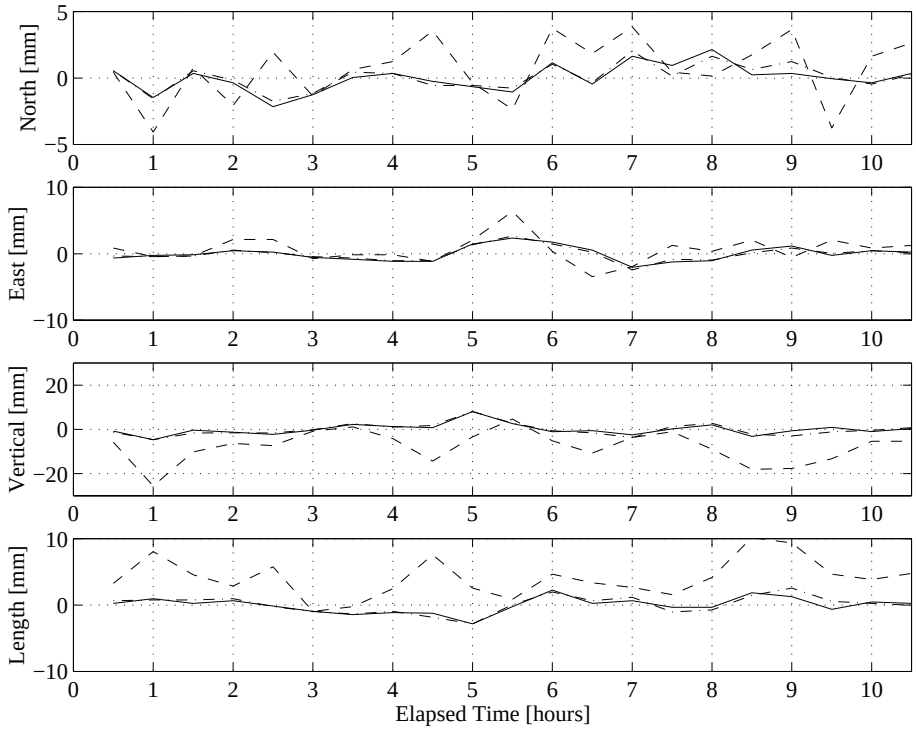

Figure 5. Repeated solutions of baseline D3-DT; length of sessions = 30 minutes.

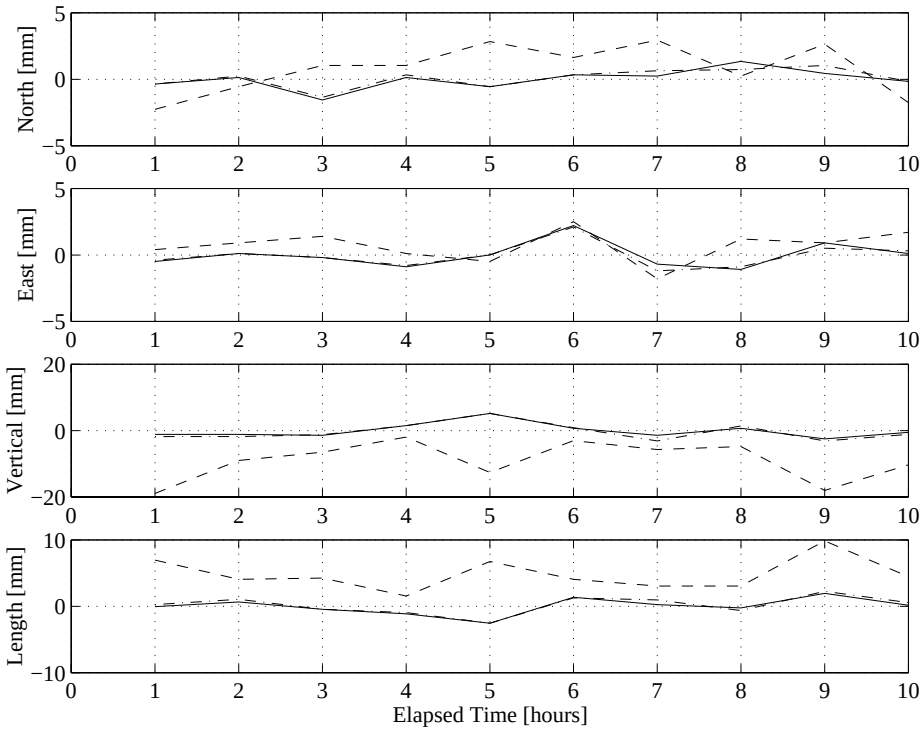

Figure 6. Repeated solutions of baseline D3-DT; length of sessions = 60 minutes.

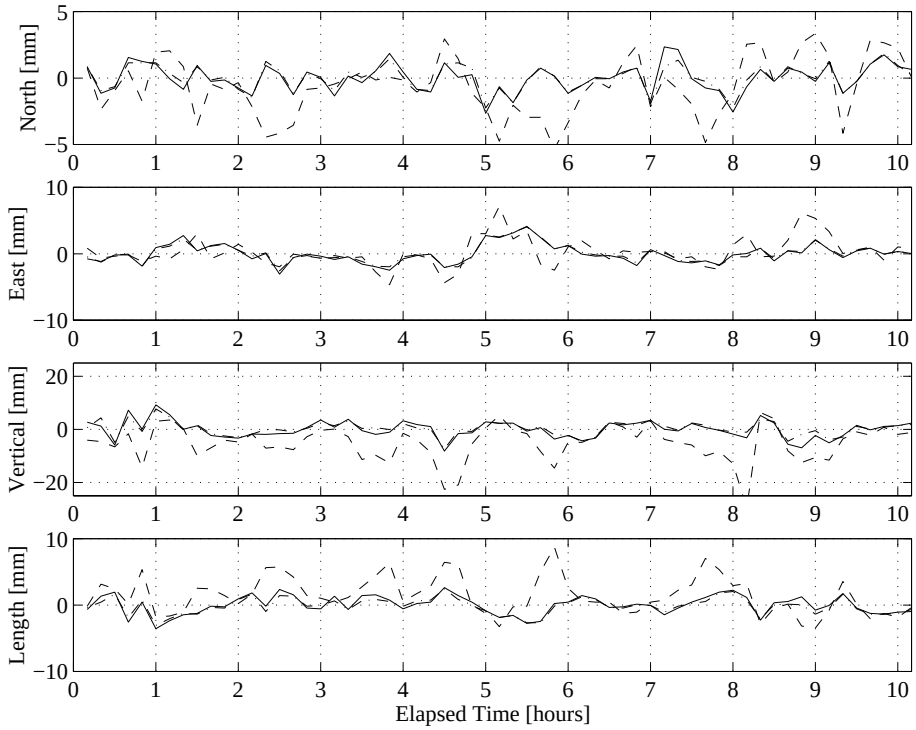

Figure 7. Repeated solutions of baseline D3-UT; length of sessions = 10 minutes.

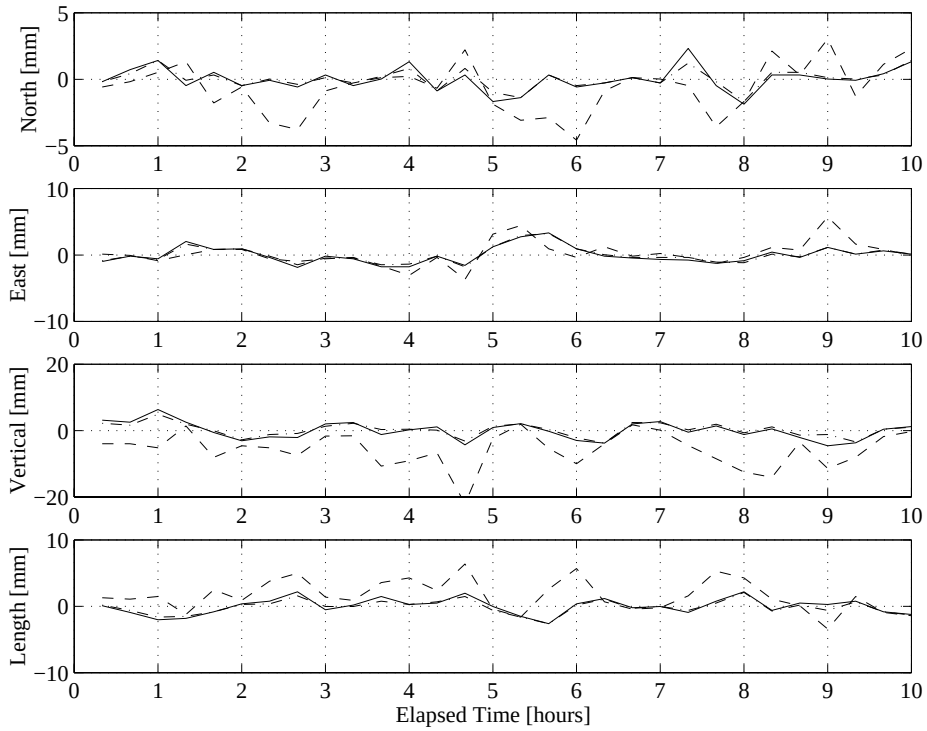

Figure 8. Repeated solutions of baseline D3-UT; length of sessions = 20 minutes.

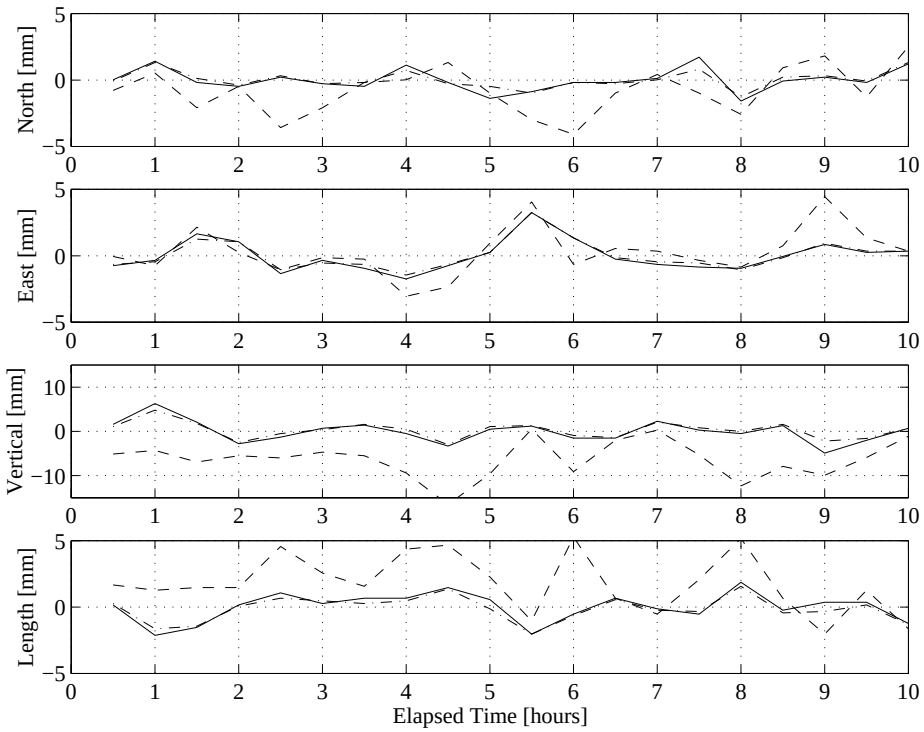

Figure 9. Repeated solutions of baseline D3-UT; length of sessions = 30 minutes.

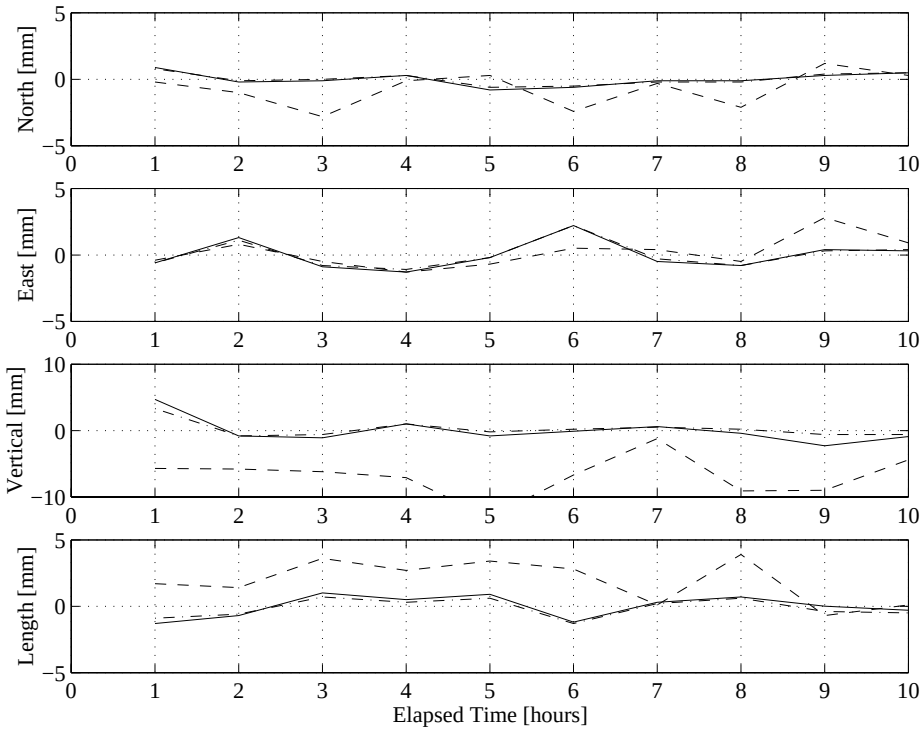

Figure 10. Repeated solutions of baseline D3-UT; length of sessions = 60 minutes.

The first immediate result is that the cosecant and SNR weighted solutions are more consistent from session to session irrespective of the actual session length. The range of the discrepancies between the equal-weight solutions and the cosecant and SNR weighted solutions can reach the 1 cm level for all the position components and even the 2 cm level for the vertical component. Given the nature of our weighting schemes we can attribute these differences to the impact of multipath. It is interesting to note that the coordinate discrepancies computed by the two new weighting schemes are almost indistinguishable. We shall examine this in more detail shortly.

In general, as we increase the session lengths, the range of discrepancies between the solution types decreases, as we would expect given progressively longer integration times. However, vertical discrepancies for the equal-weight solutions can still be at the 1 cm level and even 2 cm for the D3-DT baseline. The equal-weight solutions with the 60 minute integration times have an almost constant vertical bias compared to the other two solutions.

The variations in the coordinate discrepancies seen in Figure 3 to Figure 10 can be described using the short-term repeatability (STR) statistic. This is a common measure of GPS performance, used to indicate the scatter of a set of solutions, assuming that each one is independent. The short-term repeatability is defined as the weighted root-mean-square scatter about the weighted mean of each baseline component [*Dixon*, 1991]:

$$STR_c^2 = \frac{n}{n-1} \frac{\sum_{i=1}^{n} \frac{(c_i - \bar{c})^2}{\sigma_{c_i}^2}}{\sum_{i=1}^{n} \frac{1}{\sigma_{c_i}^2}} \qquad (2)$$

where c_i is the estimate of the particular baseline component (north, east, vertical or length) from session *i*, *n* is the number of sessions for which solutions were computed, $\bar{c}$ is the weighted average of the component estimated from all the sessions, and σ_{c_i} is the component formal error from session *i*. Given the short baselines processed in this study, equation (2) will primarily show variations due to the unmodelled effects of multipath and noise.

Figure 11 and Figure 12 show the short-term repeatability of the two cross-section baselines. The same results are reproduced numerically in Table 3 and Table 4. From these results we can see that all three types of weighting function provide solutions with sub-centimetre level vertical repeatability for even the shortest session length. However, the results for the cosecant and SNR weighted solutions are at the several-millimetre level for all the position components and sessions lengths. In general, the new weighted solutions show much less variation with respect to the session length than for the equal-weight solutions. It is interesting to note that the cosecant weighting scheme produces a consistently slightly higher repeatability than the SNR weighting scheme for all the components of baseline D3-UT and for the eastings of baseline D3-DT. Otherwise the results of the two weighting schemes are again highly consistent with each other.

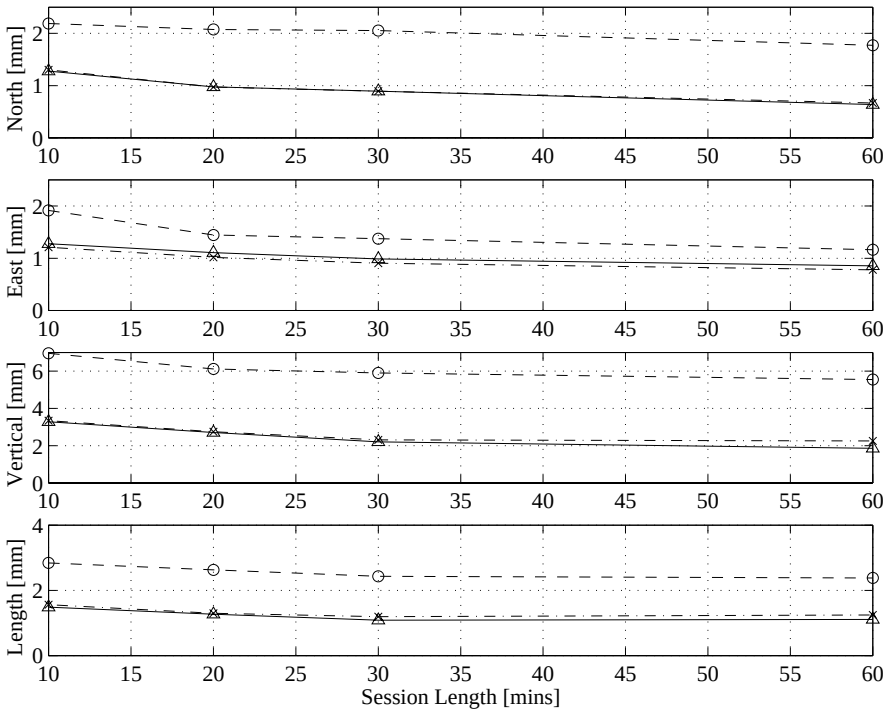

Figure 11. Short-term repeatability of station DT solutions.
Equal-weights (○); cosecant weights (×); SNR weights (Δ).

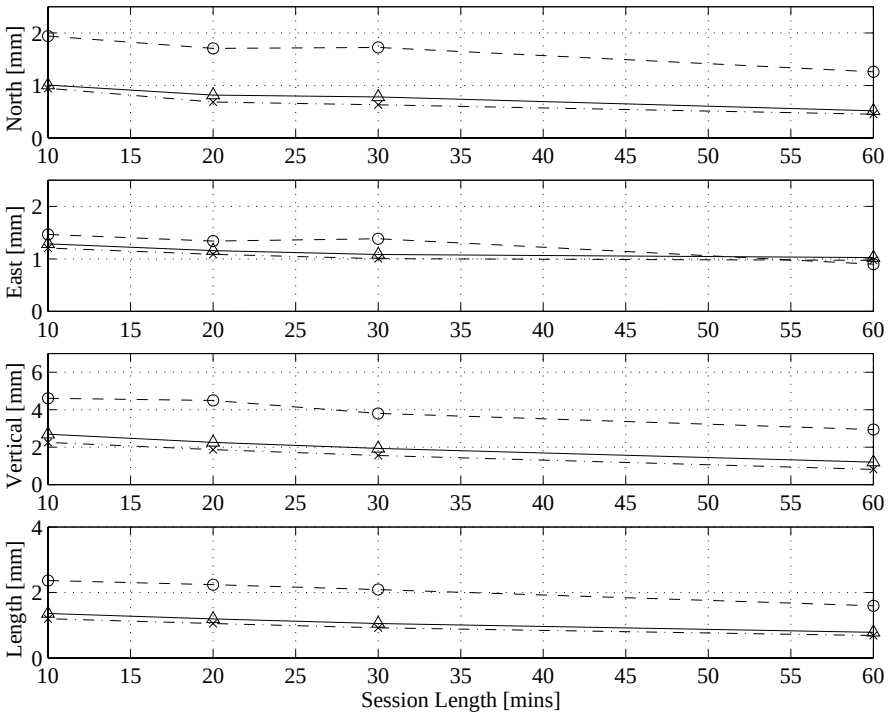

Figure 12. Short-term repeatability of station UT solutions.
Equal-weights (○); cosecant weights (×); SNR weights (Δ).

Table 3. Coordinate repeatability (mm); station DT.
Results per session length for equal-, cosecant- and SNR-weights respectively.

Session Length	North	East	Vertical	Length
10 Minutes	2.19	1.92	6.96	2.84
	1.30	1.21	3.34	1.56
	1.28	1.28	3.28	1.49
20 Minutes	2.07	1.44	6.12	2.63
	0.97	1.02	2.75	1.30
	0.98	1.11	2.71	1.27
30 Minutes	2.05	1.37	5.90	2.43
	0.89	0.91	2.31	1.20
	0.89	0.99	2.21	1.09
60 Minutes	1.77	1.16	5.55	2.38
	0.67	0.78	2.26	1.25
	0.64	0.86	1.86	1.11

Table 4. Coordinate repeatability (mm); station UT.
Results per session length for equal-, cosecant- and SNR-weights respectively.

Session Length	North	East	Vertical	Length
10 Minutes	1.94	1.46	4.61	2.37
	0.95	1.21	2.26	1.20
	1.01	1.29	2.69	1.36
20 Minutes	1.71	1.34	4.50	2.24
	0.68	1.09	1.87	1.06
	0.82	1.16	2.25	1.20
30 Minutes	1.72	1.38	3.80	2.09
	0.63	1.01	1.56	0.92
	0.78	1.08	1.94	1.05
60 Minutes	1.26	0.90	2.94	1.59
	0.45	0.97	0.81	0.69
	0.52	1.03	1.21	0.78

These simple repeatability statistics do not tell the whole story, however. As we saw in the discrepancy plots, there is a wide variation in the range of the estimated coordinate components. The STR statistics may be masking some solutions that should be treated as outliers. To quantify this, we can examine plots of the cumulative short-term repeatability. Figure 13 and Figure 14 show the cumulative short-term repeatability for the 10 minute sessions of stations DT and UT. The final cumulative values at the right-hand side of each plot are the 10 minute values plotted in Figure 11 and Figure 12.

What these plots show is that on the whole, repeatability does improve for all the weighting techniques as more solutions are computed. However, for the vertical component of station DT, an increase in the repeatability of the new weighted solutions is visible at approximately the 30^{th} session. The cumulative repeatability increases from a minimum of 2.6 mm to 4.1 mm in only six sessions and then decreases to the final value of 3.3 mm. A similar increase occurs in the north and length components at the 34^{th} session. While small, these changes point to the fact that there are some sessions that could be eliminated to improve the overall repeatability. If the number and length of observation sessions that can be made are limited for economic or other reasons, then some pre-planning may be required to identify the best times to take observations for particular sites. However, we need to identify the reason why some sessions are worse than others.

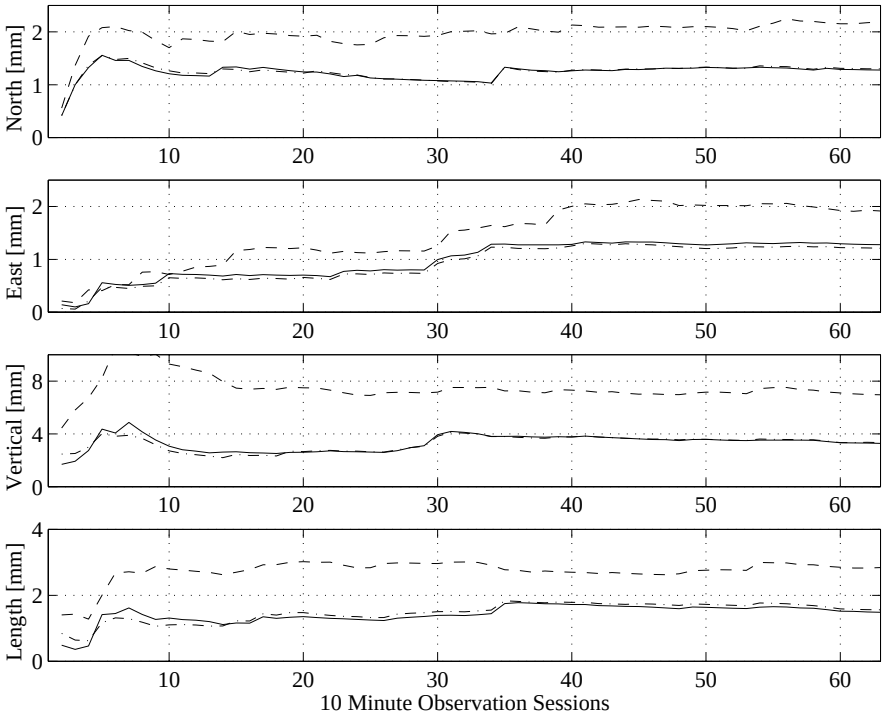

Figure 13. Cumulative short-term repeatability of station DT solutions. Equal-weights (– –); cosecant weights (– ·); SNR weights (—).

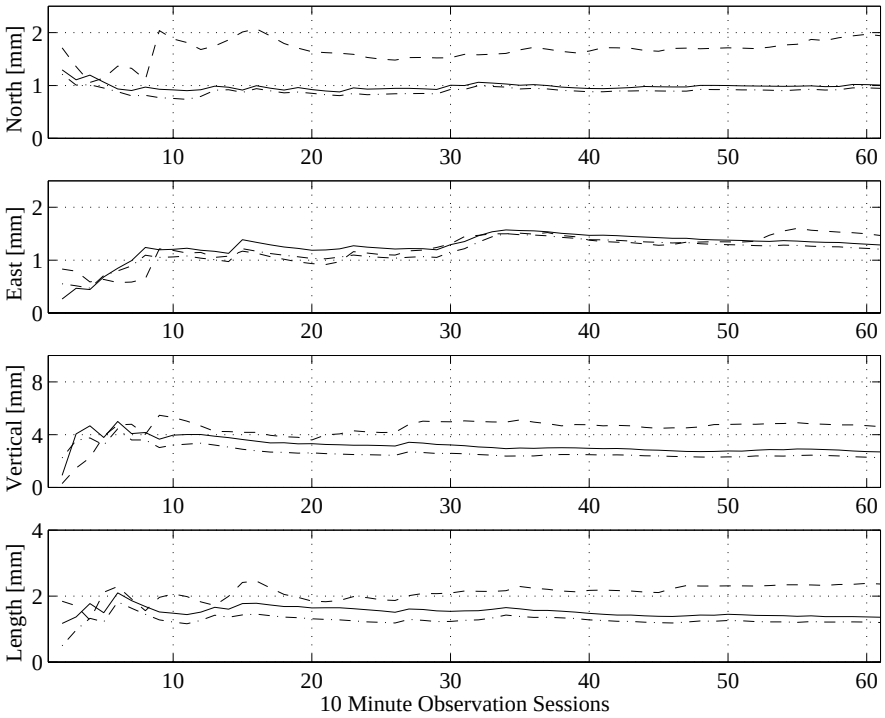

Figure 14. Cumulative short-term repeatability of station UT solutions. Equal-weights (– –); cosecant weights (– ·); SNR weights (—).

These repeatability results have also highlighted the fact that the results for station DT are consistently worse than for station UT, although the cosecant and SNR weighting schemes appear to reduce the effect to the several millimetre level (in the vertical component). Given that observations from station D3 are common to both baselines, it would appear that station DT is in a more multipath-prone environment than station UT.

If we consider the residual plots in Figure 15, we can see that the dispersion of the residuals does not appear to be significantly different for either baseline. Both baselines do appear to have significant variations in the residuals with patterns that are normally indicative of multipath. The residuals for baseline D3DT do appear to have more outliers, some of which correlate well with large vertical discrepancies in the equal weight solutions in Figure 3 (cf. at 1 and 9 hours).

Another limitation on the solution accuracy is usually the satellite constellation geometry. The elevation angles of the satellite constellation common to both stations of both baselines are plotted in Figure 16. It is immediately apparent that there is very little data below 20° for the D3-DT baseline. This is reinforced in Figure 17, where the actual number of satellites and corresponding HDOPs can be compared between both baselines. The general trends are the same, but there are significant periods of time when there are one, or even two, fewer satellites available on the D3DT baseline than for D3UT.

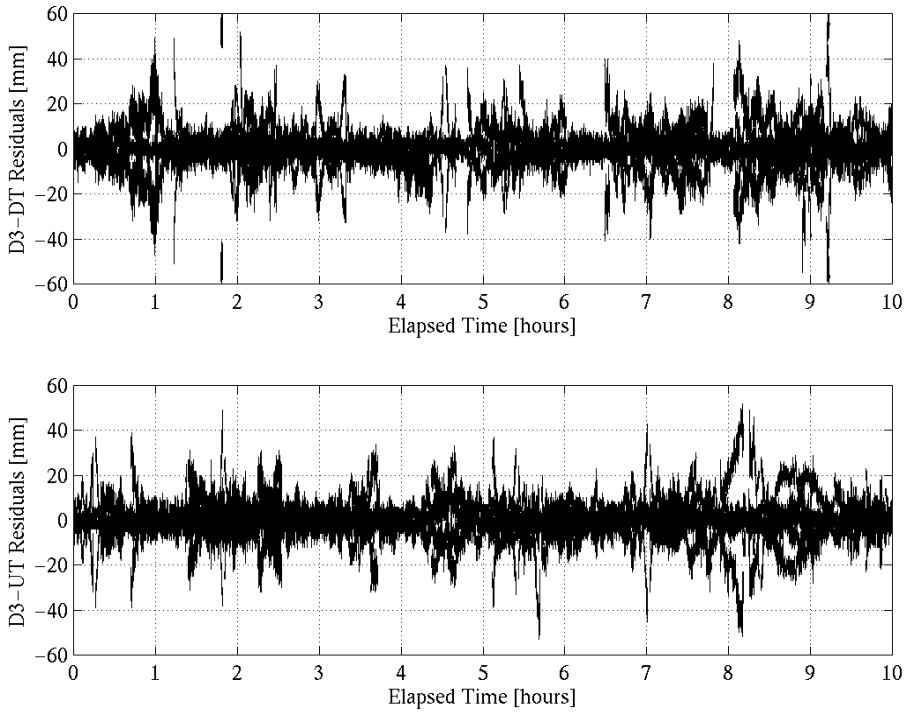

Figure 15. L1 double-difference carrier phase residuals from the SNR weighted control solutions for baselines D3-DT and D3-UT respectively.

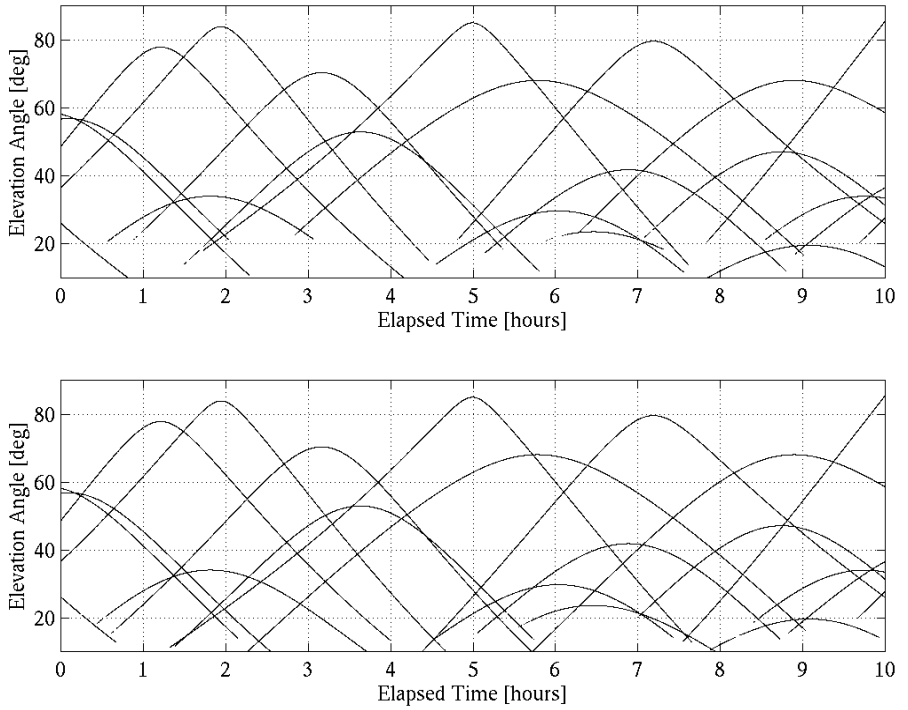

Figure 16. Satellite constellation for baselines D3-DT and D3-UT respectively.

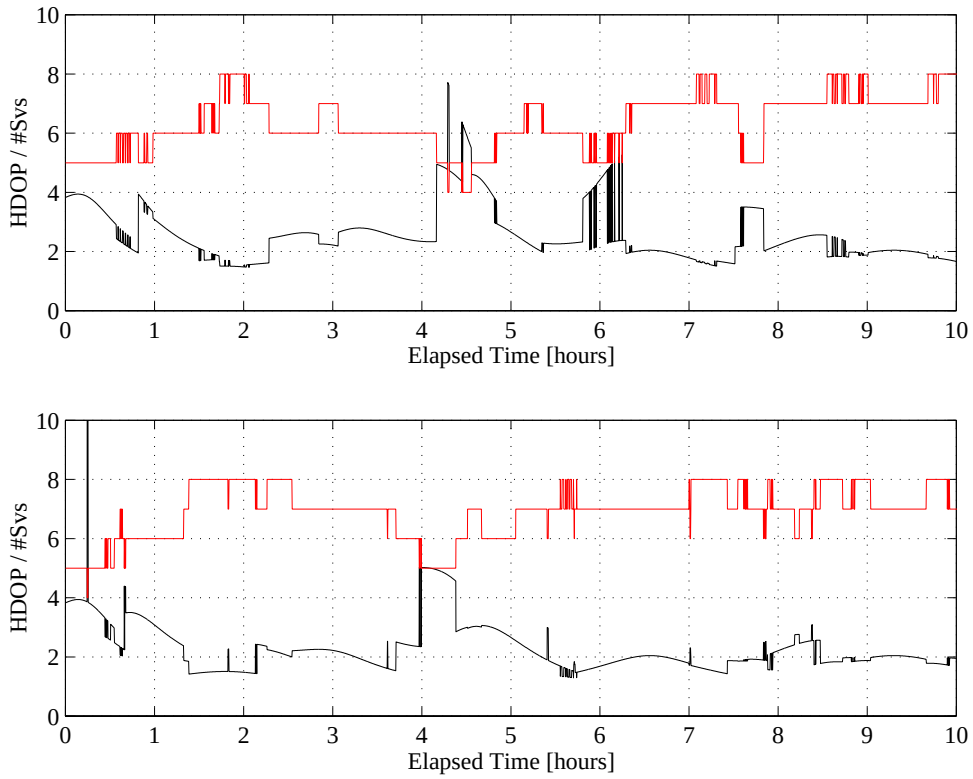

Figure 17. Satellite count and HDOP for baselines D3-DT and D3-UT respectively.

Some of these periods of poorer geometry can be correlated with some of the larger formal errors in the vertical and length components of the two baselines and for the standard deviations of the residuals (Figure 18 and Figure 19). There are several sessions on both baselines where the standard deviation for the equal-weight solution residuals is considerably smaller than for the other two weighting schemes. This suggests that the coordinates are absorbing some of the multipath and that the formal error is particularly optimistic for these sessions. On the whole the cosecant and SNR weighted solutions show less variation in the formal errors across all the sessions.

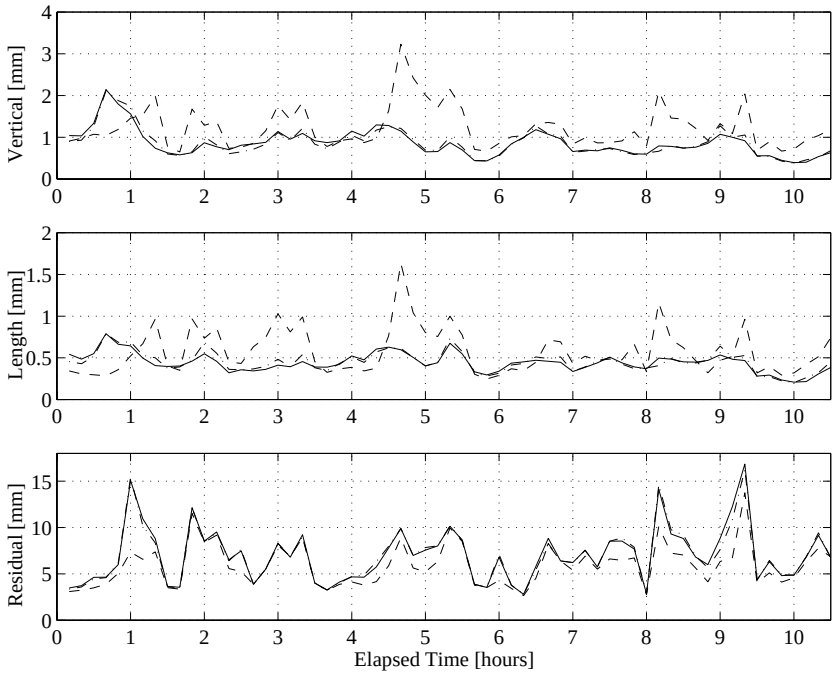

Figure 18. Formal errors (3σ) of the vertical and length components and standard deviations of the residuals of the ten minute session results from baseline D3-DT. Equal-weights (– –); cosecant weights (– ·); SNR weights (—).

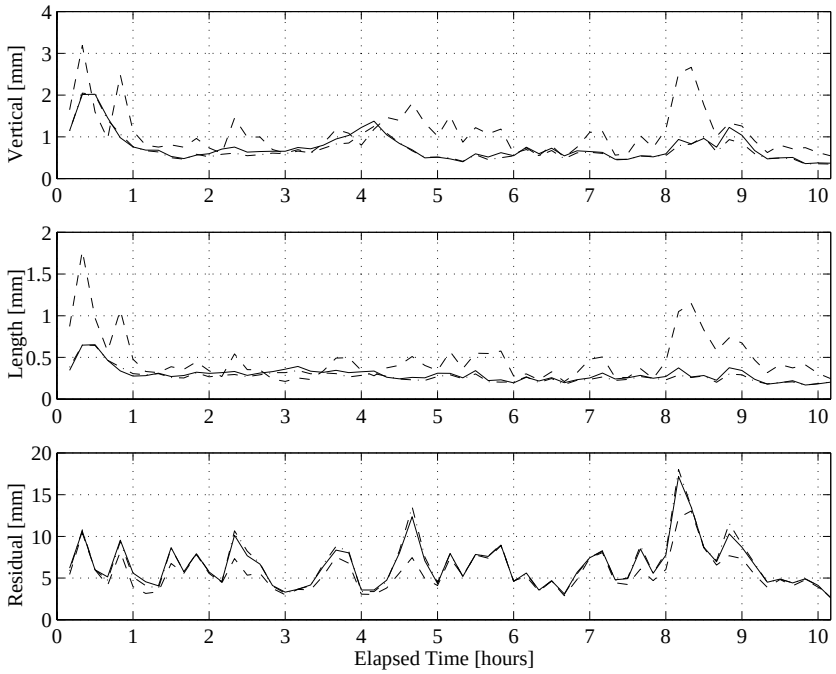

Figure 19. Formal errors (3σ) of the vertical and length components and standard deviations of the residuals of the ten minute session results from baseline D3-UT. Equal-weights (– –); cosecant weights (– ·); SNR weights (—).

2.3. Resolving Ambiguities

As was mentioned previously, all the repeatability results used carrier phase ambiguity values fixed from the control solutions. In general practice, this will obviously not be possible if data is only collected over short observation sessions. We therefore ran the 10 minute sessions in a 'float ambiguity' mode to estimate the integer values. Each baseline was processed with the same *a-priori* coordinates, but with different *a-priori* uncertainties. The estimated ambiguity values were rounded to the nearest integer (regardless of actually how close they were to an integer) and compared with the correct values. The results are summarised in Table 5.

Table 5. Number of sessions with incorrect ambiguities using different *a-priori* coordinate constraints (σ_{llh}) for stations DT and UT.

Baseline	Wgt. Scheme	σ_{llh} = 1 cm	σ_{llh} = 5 cm	σ_{llh} = 10 cm
D3-DT	Equal wgt.	0	23	26
	Cosecant wgt.	0	0	0
	SNR wgt.	0	0	0
D3-UT	Equal wgt.	0	20	26
	Cosecant wgt.	0	0	0
	SNR wgt.	0	0	0

Table 5 clearly shows the influence of the new weighting schemes on the ambiguity resolution process. For short observation sessions with equal weighting of the observations, the a-priori coordinates must be very accurate to guarantee that the correct

ambiguities will be estimated. However, the use of cosecant or SNR weights allows for coordinates with a greater amount of uncertainty.

2.4. Weighting Scheme Equivalence

Throughout the presentation of these results we have seen that the coordinate estimates derived using the cosecant and SNR weighting schemes have been almost equivalent. The reason for this can be understood by examining Figure 20. This shows single-receiver observation variances computed using the cosecant and SNR weighting schemes (the SNR data is from station D3). The SNR variances have been multiplied by a constant factor (10^3) to align them approximately with the cosecant variances. This is equivalent to changing the *a-priori* variance factor, which does not change the parameter estimates of a least-squares solution. Correspondingly, all the constant terms in equation (1) can be thought of as being part of the *a-priori* variance factor and as such their influence will be scaled out by the *a-posteriori* variance factor. Hence, it is not necessary to specify the correct receiver bandwidth, or even the cycles-to-metres conversion factor when computing the SNR weights, because they are all constant values.

Figure 20 also indicates that the function $1/\tan^2(e)$ may also be a suitable weighting scheme should SNR values not be available. A slight adjustment to the formula would have to be implemented to avoid the singularity $\tan(90°) = 0$, however using $1/\tan^2(e–0.1°)$ should be more than adequate. Alternatively, exponential functions might also prove useful.

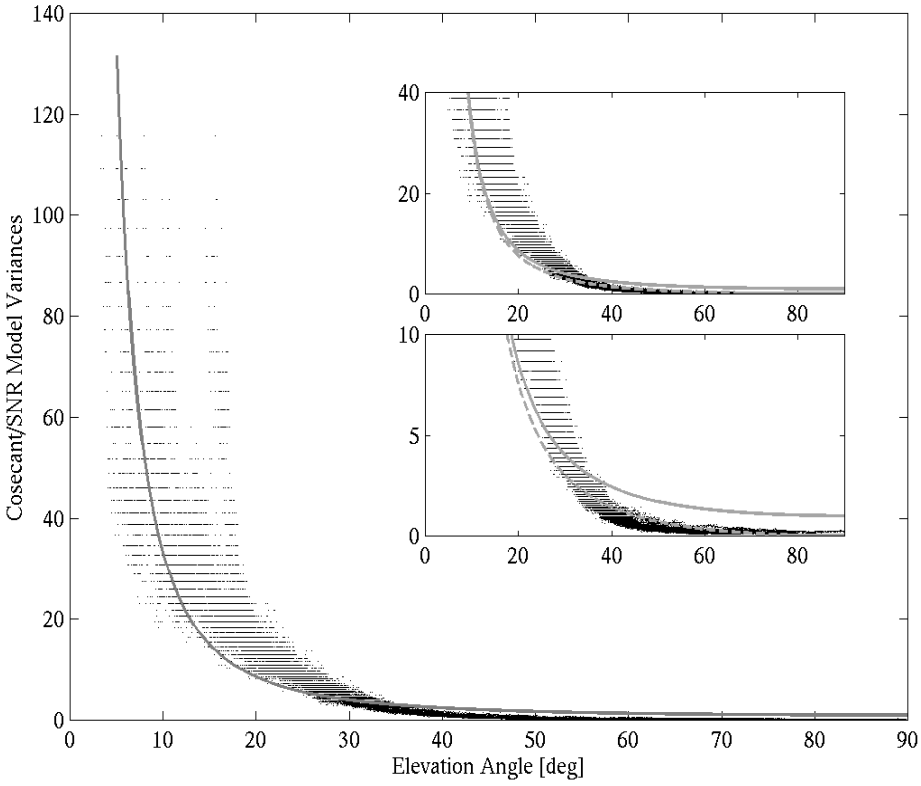

Figure 20. Inverse weights computed by the cosecant (—) and SNR weighting schemes (·). The SNR data is from station D3; the dashed line in the inset plots represents $1/\tan^2(e)$.

3. SUMMARY AND CONCLUSIONS

We have implemented several observation weighting schemes into our sequential least-squares GPS data processing package DIPOP. The effectiveness of these weighting schemes has been evaluated with a large set of GPS data recorded at an earth dam structure monitored by the U.S. Army Corps of Engineers. The first weighting scheme is the standard scheme that applies equal weights to all the carrier phase observations. The second scheme uses the cosecant of the elevation angle (equivalent to the tropospheric delay mapping function) in computing the a-priori weight and the third scheme uses the signal-to-noise values as output by Trimble GPS receivers.

Our results have highlighted the complex nature of several error sources when trying to compute very precise, very accurate, coordinates using GPS data. Both the second and third weighting schemes have reduced the impact of multipath on coordinate differences to an average level of several millimetres. There remain some short sessions however, where the vertical coordinate differences between individual solutions and weighting schemes approaches the 1 cm level. This suggests that if GPS data can only be recorded for short sessions at a time, those time periods will have to be chosen carefully to minimise the impact of multipath and the satellite geometry. Even then, there are no guarantees that one or two satellites might not fail or be unavailable at that particular time and irreparably degrade the solution accuracy. The only solution to this dilemma would be to increase the length of the observation sessions to something approaching 30 minutes to provide as much data redundancy as possible.

We observed very little difference between results obtained using the cosecant weighting function and the SNR weighting function when processing this data. This could be due to two factors. The "SNR counts" output by the Trimble receivers are not true C/N_0 values. However, they do mimic the general trends of real C/N_0 values, and it is the relative noise between observations that is important for the variance-covariance matrix of the least-squares technique. What is more likely is that the "first order" noise effects on the GPS carrier phase observations are due to the antenna gain pattern, which can be suitably mimicked by the cosecant function of the satellite elevation angle. The quasi-sinusoidal variations of the SNR due to multipath seem to occur over time-scales shorter than the solution integration times we have used here.

With regard to occupation times, resolving ambiguities for short observation sessions should not be a problem provided that the station coordinates are already known to a fairly high accuracy. The use of a good weighting scheme increased the allowable *a-priori* coordinate uncertainty from the 1 cm to level to the 10 cm level for the data processed here. *A-priori* coordinates such as these could be derived from long-period 'reference data sets', recorded at monitoring sites as a precursor to the monitoring of a structure with GPS. These reference data sets could also give an indication as to what problems may be expected due to multipath and satellite geometry at each station. Computing the short-term repeatability statistics would give an indication of the expected uncertainty for any single subsequent re-occupation and hence the level of movement that could be detected in the structure being monitored.

As an alternative to using reference data sets, it may be possible to use real-time kinematic (RTK) techniques, to obtain concurrent estimates of the position accuracy. With this technique, points could be occupied for as long as necessary to achieve a required accuracy. If independent measurements can be made of the baseline lengths and relative heights of the East Lynn network, by conventional geodetic techniques for example, both the data processed here, and the un-processed rapid-static sessions could be used to simulate and investigate this technique.

REFERENCES

anon. (1998). "Possible future changes of the RINEX format" http://igscb.jpl.nasa.gov:80/igscb/data/format/future.txt [last modified: 05-Oct-95].

Axelrad, P., C. Comp and P. MacDoran (1994). "Use of signal-to-noise ratio for multipath error correction in GPS differential phase measurements: Methodology and experimental results." *Proceedings of ION-GPS'94*, Salt Lake City, Utah, 20-23 September, pp. 655-666.

Braasch, M.S. and A.J. Van Dierendonck (1999). "GPS receiver architectures and measurements." *Proceedings of the IEEE*, Vol. 87, No.1, pp. 48-64.

Black, H.D. and A. Eisner (1984). "Correcting satellite doppler data for tropospheric effects." *Journal of Geophysical Research*, Vol. 89, No. D2, pp. 2616-2626.

Comp, C.J. and P. Axelrad (1996). "An adaptive SNR-based carrier phase multipath mitigation technique." *Proceedings of ION-GPS'96*, Kansas City, Mo., 17-20 September, pp. 683-697.

Dixon, T.H. (1991). "An introduction to the Global Positioning System and some geological applications." *Reviews of Geophysics*, Vol. 29, No. 2, pp. 249-276.

Estey, L.H. (1998). Personal communication. UNAVCO, Boulder, Colorado, September.

Hartinger, H. and F.K. Brunner (1998). "Attainable accuracy of GPS measurements in engineering surveying." *Proceedings of the F.I.G. XXI International Congress, Commission 6*, Brighton, U.K., 19-25 July, pp. 18-31.

Herring, T.H. (1998). *GPS noise analysis using signal-to-noise ratio (SNR) analysis: Software and example*. http://bowie.mit.edu/~tah/snrprog/ [last modified: 16-Aug-98].

Langley, R.B. (1997). "GPS receiver system noise." *GPS World*, Vol. 8, No. 6, pp. 40-45.

Talbot, N. (1988). "Optimal weighting of GPS carrier phase observations based on the signal-to-noise ratio." *Proceedings of the International Symposia on Global Positioning Systems*, Queensland, Australia, 17-19 October, pp. V.4.1-V.4.17.

Tiberius, C., N. Jonkman and F. Kenselaar (1999). "The stochastics of GPS observables." *GPS World*, Vol. 9, No. 2, pp. 49-54.

APPENDIX A. MODIFICATIONS TO THE DIPOP GPS SOFTWARE

Modifications to the DIPOP software were twofold: 1) extra code was required to pass the SNR values through the pre-processor PREGO and into PREDD, where they are converted to sigma noise values using equation (1); and 2) extra code was required in the main processor MPROC to read the noise values associated with the observations and to compute the observation weight matrix every epoch, instead of once per session for equal weighting and mathematical correlation's only.

The SNR weights computed by PREDD are stored as single difference standard deviations in the double difference observation files. This allows for easier handling should an observation be deleted because of a change in the elevation angle cut-off mask or if requested by the user. It is also easier to form the double-difference variance-covariance matrix, as we will show here.

DIPOP uses the matrix operator J to form the double difference observable vector $\nabla\Delta\Phi$ from the between-receiver single difference observable vector $\Delta\Phi$:

$$\nabla\Delta\Phi = \mathrm{J} \cdot \Delta\Phi \quad , \tag{A1}$$

where $\mathrm{J} = \begin{bmatrix} 1 & -1 & 0 & 0 & \dots & 0 & 0 \\ 0 & 1 & -1 & 0 & \dots & 0 & 0 \\ \vdots & & & & & & \vdots \\ 0 & 0 & 0 & 0 & \dots & 1 & -1 \end{bmatrix}$. Applying the law of variance-covariance propagation to the covariance matrix of the single differences $C_{\Delta\Phi}$, we get:

$$C_{\nabla\Delta\Phi} = J \cdot C_{\Delta\Phi} \cdot J^{T} \quad . \qquad (A2)$$

Computing $C_{\nabla\Delta\Phi}$ in this way automatically takes into account the mathematical correlations introduced by using the double-difference observables. When using equal weights for all observations, $C_{\Delta\Phi} = \sigma_0^{\,2}\, I$, where I is the identity matrix and $\sigma_0^{\,2}$ is the *a-priori* variance factor specified by the user. Equation (A2) then gives:

$$C_{\nabla\Delta\Phi} = \sigma_0^{\,2} \begin{bmatrix} 2 & -1 & 0 & 0 & 0 \\ -1 & 2 & -1 & 0 & 0 \\ 0 & -1 & 2 & -1 & 0 \\ \vdots & & & \ddots & \\ 0 & 0 & 0 & -1 & 2 \end{bmatrix} .$$

When using a vector of individual variances for each single difference, $C_{\Delta\Phi} = diag([\sigma_1^2,\ \sigma_2^2,\ \ldots\ \sigma_n^2]^T)$, equation (A2) gives:

$$C_{\nabla\Delta\Phi} = \begin{bmatrix} \sigma_1^2 + \sigma_2^2 & -\sigma_2^2 & 0 & 0 & 0 \\ -\sigma_2^2 & \sigma_2^2 + \sigma_3^2 & -\sigma_3^2 & 0 & 0 \\ 0 & -\sigma_3^2 & \sigma_3^2 + \sigma_4^2 & -\sigma_4^2 & 0 \\ \vdots & & & \ddots & \\ 0 & 0 & 0 & -\sigma_{n-1}^2 & \sigma_{n-1}^2 + \sigma_n^2 \end{bmatrix} ,$$

where *n* is the number of single difference observations. This immediately shows the suitability of working with the single difference variances. The double difference weight matrix follows from:

$$P_{\nabla\Delta\Phi} = C_{\nabla\Delta\Phi}^{-1} . \qquad (A3)$$